FRET enabled light harvesting within quantum dot loaded nanofibers

FRET enabled light harvesting within quantum dot loaded nanofibers

Yemliha Altıntas,[1] Nuri Burak Kiremitler,[2, 3] Sinan Genç,[4] M. Serdar Onses,[2, 3*] Evren Mutlugün[4*]

[1] *Department of Materials Science and Nanotechnology, Abdullah Gül University, Kayseri, Turkey TR-38080.*
[2] *Department of Materials Science Engineering, Erciyes, Kayseri, Turkey TR-38039.*
[3] *Nanotechnology Research Center (ERNAM) Erciyes University, Turkey TR-38039*
[4] *Department of Electrical-Electronics Engineering, Abdullah Gül University, Kayseri, Turkey TR-38080.*
*Corresponding authors *evren.mutlugun@agu.edu.tr, onses@erciyes.edu.tr*

Abstract

The spatial control of the nano-emitters in novel light harvesting platforms offers great potential for the manipulation of the excitonic interaction amongst the donor-acceptor pairs of energy transferring agents. In this work, we report colloidal quantum dot loaded electrospun nanofibers as a light harvesting platform to study the excitonic interaciton among them. The donor emission lifetime modified from 12.46 ns to 7.45 ns with the change in the ratio of green and red quantum dots in the nanofiber, as a result of confining acceptor quantum dots in close proximity. The spectrally narrow emitter luminescent nanofiber platforms have further been investigated for their potential of white light generation. The hybrid platform of blue LED integrated electrospun nanofibers has been shown to demonstrate a correlated color temperature (CCT) of 3632.5K, luminous efficacy of optical radiation (LER) value of 307.7 lm/W_{opt} along with color rendering index (CRI) value of 60.

Keywords: Colloidal quantum dots, photoluminescence, nanofiber, white light

1. Introduction

Semiconductor quantum dots (QDs) have been on demand for lighting and display technologies for their superior and size tunable optical properties, high luminescence efficiency and their solution processable nature [1]. In general, colloidal QDs based on II-VI and III-V materials can can generate light with high efficiency by optical or electrical pumping. Thanks to the quantum confinement, QDs possess spectrally pure emission and are being employed as active light generation agents to replace the conventional phosphor materials [2, 3]. Their narrow emission bandwidths along with finely adjusted emission peak wavelengths in the spectrum create an exclusive platform to provide novel solutions for white light generation applications [4].

Acting both in photoluminescence and electroluminescence mode, the exciton generation in colloidal QDs allows niche applications in optoelectronics [5-7]. In literature, QDs hybridized with blue inorganic light emitting diodes have been shown to reveal the potential of their white light generation. Besides being employed as an energy down converting agents with LEDs, the excitonic interaction of the colloidal particles have also attracted considerable interest for the manipulation and engineering of the light [8].

Based on a nonradiative energy transfer, the interaction of the different sized colloidal particles also provides an alternative light engineering mechanism, opening up a new channel for exciton harvesting. The energy transfer using QDs has been studied to demonstrate their excitonic interaction when placed in proximity to the donor/acceptor agents [9,10]. In order to have an efficient energy transfer, most importantly, the energy donating and accepting pairs should be in close proximity, donor emission spectrum should have a spectral overlap with the acceptor species, and donor emitter should have a high photoluminescence quantum yield. Given all the competitive optical properties, confining colloidal particles into a spatially confined regime still

remains a challenge for controlling the interaction amongst donor and acceptor pair. Embedding QDs in a polymer matrix and fabrication of their structure in a 3D network does not provide a control over their spatial confinement. There is a need for 1D nanostructures which can confine QDs in a way that the particles are located in close-proximity.

A convenient approach to fabrication of 1D nanostructures is electrospinning fibers from polymer solutions. Besides the simplicity and low cost, electrospinning presents a solution processable route to fabrication of 1D nanostructures for confinement of colloidal quantum dots [11-15]. By the right choice of polymer and solvent suitable for the ligand of QDs, it is possible to generate exotic confinement structures consisting of the particles uniformly located in the polymer fiber matrix [16]. In an effort to embed colloidal quantum dots in nanofibers, there have been previous efforts to fabricate electrospun structures to generate white light [17-18]. Choi et al. demonstrated the effect of the nanofiber diameter for control of the excitonic interaction among quantum dots [19]. However, the control of nonradiative energy transfer within the same nanofiber medium has not been demonstrated thus far.

Here, we propose and demonstrate a novel light-harvesting platform consisting of green and red emitting colloidal quantum dots loaded into nanofibers. Confining the 0D colloidal QDs in a quasi 1D nanofibers, we have intentionally changed the concentration of the donor-acceptor pairs in the same fiber structure and observed the excitonic interaction in a spatially confined regime. In this work, we have enabled an extensive investigation of the time resolved spectroscopy to reveal the emission dynamics of the colloidal particles. Furthermore, we have developed a hybridized platform of nanofiber integrated blue LEDs for white light generation. In those lines, our study provides an integrative work of synthesis of highly luminescent particles, fabrication of

QD loaded electrospun nanofibers and an investigation of the nonradiative energy transfer and generation of white light based on energy down conversion mechanism.

2. Experimental

2.1. Chemicals and Reagents:

CdSe/ZnS core shell quantum dots were carried out using cadmium oxide (CdO, 99.99%), zinc acetate (ZnAc, 99.99%), selenium (Se, 99.99% powder), sulfur (S, 99.998% trace metals basis; 99.5% purum), oleic acid (OA, 99.99% technical grade), 1-dodecanethiol (DDT, 98%)1-octadecene (1-ODE, 90% technical grade), trioctylphosphine (TOP, 97%), Ethanol (EtOH, 99.8% absolute), Acetone (Act, 99.5% absolute) and Methanol (MeOH, absolute). All chemicals and reagents were purchased from Sigma-Aldrich. EtOH and de-ionized water were used as the cleaning medium of the experimental apparatus. All chemicals were used without further purification.

2.2. Procedure for synthesis of CdSe/ZnS core shell quantum dots

2.2.1. Synthesis procedure of green emitting QDs (PL λ_{max} = 521nm)

A single injection step of precursor method was used for the synthesis of green emitting CdSe/ZnS QDs as described previously in our previous work [20]. Starting with mixing of 0.3 mmol of CdO and 4 mmol of zinc acetate (ZnAc) with 5ml of oleic acid ($C_{18}H_{34}O_2$) in a 50ml 3-necked flask, the reactions were kept under vacuum at 150 ^oC for 30min. The reaction mixture was cooled to 50^oC and 15ml of 1-ODE ($C_{18}H_{36}$) was loaded in a 50ml reaction flask with a condenser and heated to 100 ^oC under vacuum. After the reaction system is flushed with Ar gas the temperature was increased up to 300^oC to obtain the transparent mixed solution of cadmium oleate ($C_{36}H_{66}CdO_4$) and zinc oleate ($C_{36}H_{66}O_4Zn$), respectively. A mixture of 0.3 mmol of Se and 3 mmol of S were dissolved in 2ml of TOP at 30^oC with strong stirring at 800rpm for 2

hours in the glove box. Afterwards, the clear solution of Se and S in TOP was obtained and rapidly injected the mixture of (TOP-Se-S) solution into the reaction flask at 300 ^{o}C and the solution was kept for 10 min for the completion of the green CdSe/ZnS QDs. Then, the mixture was cooled to room temperature to end up the reaction. Finally, the end up of the solution is used for the purification process. A precipitation and re-dispersion method was used for the purification of QDs. The crude solution was precipitated with an excess amount of acetone ($(CH_3)_2CO$) and methanol (CH_3OH) by centrifugation at 5000 rpm for 15 min and re-dispersed the QDs with hexane.

2.2.2. Synthesis procedure of red emitting QDs (PL λ_{max} = 626nm)

The reported procedures [21-23] were modified for the synthesis of red emitting (PL λ_{max} = 626nm) CdSe/ZnS core shell QDs. Concisely, 1 mmol of CdO and 2 mmol of zinc acetate and 5ml oleic acid were added in a 50 ml three necked flask and heated to 150 ^{o}C under vacuum for 40 min. Then, the solution was cooled to 50 ^{o}C and 25ml of 1-ODE was loaded to the mixture of cadmium oleate ($(Cd(OA)_2$) and zinc oleate ($(Cd(OA)_2$) in the reaction flask. The solution was firstly heated to 80^{o}C under vacuum waited 20 min and then increased the temperature up to 300^{o}C under Ar gas. After, we prepared the stock solution of TOP-Se with 0,2 mmol Se in 0.2 ml volume of TOP were loaded in the 4 ml vial under the strong stirring at 800 rpm for 1 hour in the glovebox. From the stock solution of TOP-Se, we took 0.2 ml and rapidly injected in the reaction flask at the elevated temperature (300^{o}C) and kept for 60 seconds. Then, 0.3ml of 1-DDT ($CH_3(CH_2)_{11}SH$) in 1ml of 1-ODE was gently injected into the system, and the reaction continued for 20min. After, 2mmol sulfur in 1ml of TOP prepared in the glovebox and this solution was slowly injected at 300^{o}C over a period of 10 min. Subsequently, the solution was cooled to room temperature in order to produce the red emitting CdSe/ZnS QDs and further used for the

purification process. The QDs solution was precipitated with the excess amount of acetone and methanol by centrifugation at 5000 rpm for 15 min and finally re-dispersed the QDs in hexane.

The quantum efficiency is calculated by comparing the emission intensity of the QDs with organic dye, Rhodamine 6G (for green emitters), or Sulforhodamine (for red emitters) with quantum efficiency of 95% and 90% in absolute ethanol, respectively, using the Eqn.1.[12]

$$QE_{sample}=QE_{ref-dye}\ \frac{I_{sample}}{I_{ref-dye}}\left(\frac{n_{sample}}{n_{ref-dye}}\right)^2 \quad (1)$$

Here *"I"* represent the integrated photoluminescence intensity when the reference dye and sample has been excited at the same excitation wavelength (extracted from the intersection point at the absorbance curves). When measuring the quantum yield, the concentration of the solutions have been adjusted as not to exceed 0.1-0.2 to prevent reabsorption and excitation wavelength (thus the absorbance intersection) has been chosen as to be appropriate range for the excitation of the reference dyes to prevent misleading interpretation.

2.3. Preparation of electrospinning solutions

Dry powders of red and green QDs were added in 1.25 mL of a mixture of solvents tetrahydrofuran and N,N-Dimethylformamide (4:1 v/v). This solution was then mixed for 3 h at room temperature using a magnetic stirrer. 0.12 g (% 9.5 g/mL) polycaprolactone (M_W = 80,000 g/mol) powder was then added to this solution and mixed until the dissolution of the entire polymer.

2.4. Electrospinning of nanofibers

The solutions containing QDs and polymer were electrospun using a commercial electrospinner (Holmarc). The solutions were placed in a 2.5 mL syringe fitted with a blunt end 18 gauge metallic needle. The syringe was placed in a horizontal configuration against a grounded collector consisting of an aluminum plate (120 mm × 280 mm). Electrospinning was performed

on glass slides mounted on the collector via a carbon tape for the ease of subsequent characterization steps. The tip-to-collector distance was kept constant at 25 cm and the feed rate of the solution was adjusted as 1-1.5 mL/h via a syringe pump. The voltage bias between the needle and collector was fixed at 15 kV.

2.5. Characterizations

Photoluminescence characterizations and UV-Vis spectroscopy were performed using Agilent-Cary Eclipse fluorescence spectrophotometer and UV-Vis spectroscopy Thermo Genesys 10S spectrometer respectively. Time correlated single photon counting measurements were carried out using Pico Quant FluoTime 200 equipped with 375nm pulsed laser diode, TEM images were taken by using FEI Tecnai G2 F30, and XPS measurements were conducted using Thermo Scientific K-Alpha X-ray Photoelectron Spectrometer System. The fibers were imaged with a SEM (Zeiss EVO LS10) following a conductive coating.

3. Results and discussion

Figure **1** presents the photoluminescence, absorption, photoluminescence excitation and time resolved photoluminescence spectra of the synthesized green and red QDs. In order to achieve a pair of highly efficient green and red quantum dots as a FRET pair, changing the reaction time and precursors concentrations, a series of synthesis were performed. These results and experimental conditions were included in the Supporting Information. The optimization of the synthesis methodology yields green and red QDs have a peak emission wavelength of 521 nm and 626 nm along with 90% and 75% photoluminescence quantum yield, respectively, in comparison with the reference organic dyes (e.g. Rhodamine 6G and Sulforhodamine). The amplitude weighted lifetimes (fit by two exponentials) of the green and red emitting quantum

dots are 19.1 ns and 23.6 ns respectively. The X-ray diffraction spectra, X-ray photoelectron spectra and transmission electron microscopy image are given in Supplementary Data file.

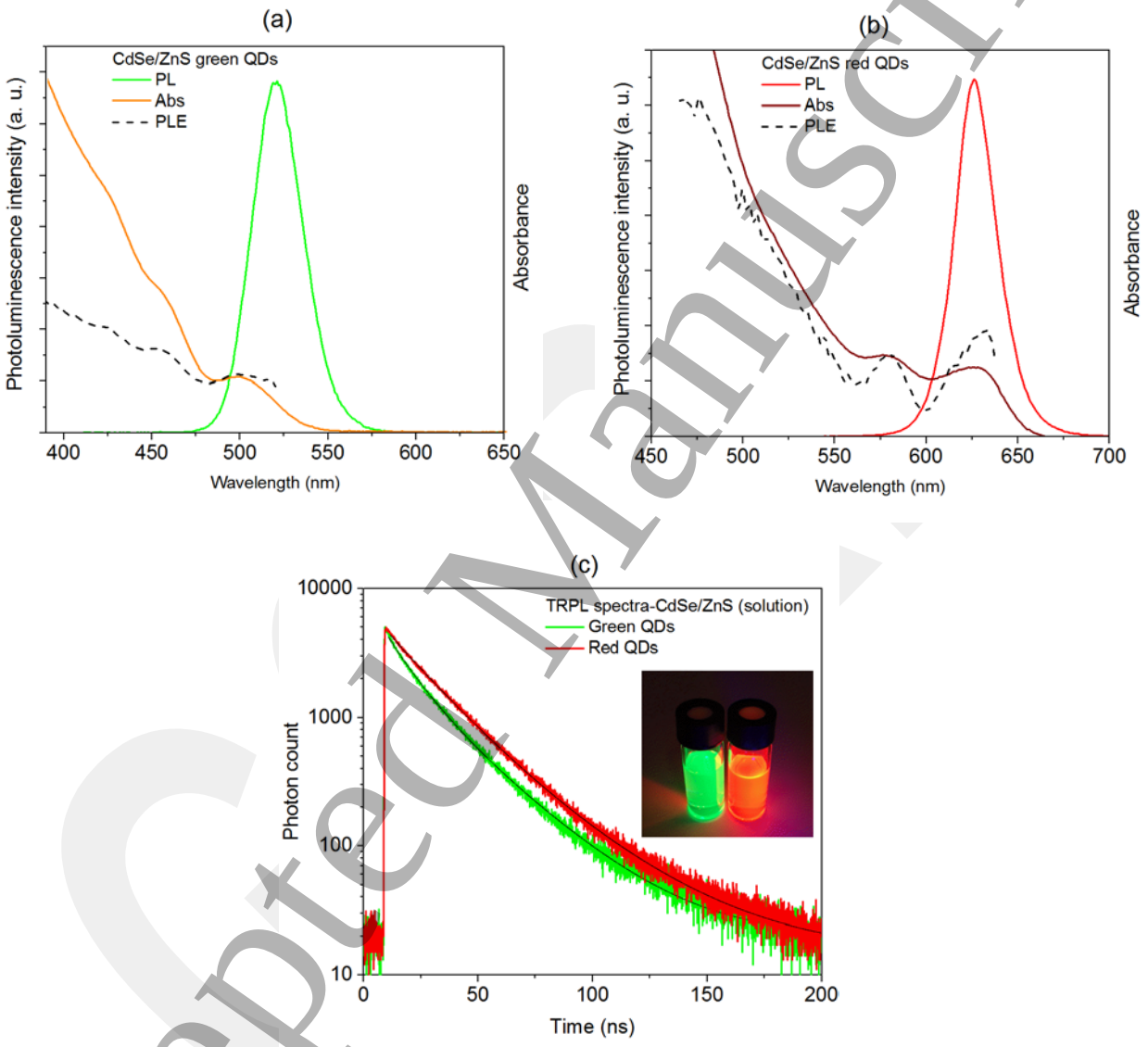

Figure 1. Photoluminescence (PL), photoluminescence excitation (PLE) and absorption spectra (Abs) of (a) green QDs, (b) red QDs, c) time resolved photoluminescence spectra for CdSe/ZnS QDs in solution.

The nanofibers were fabricated by electrospinning from a solution containing polymer and QDs. The solutions were prepared by mixing predetermined amount of the QDs in powder form

(figure **2**(a)) with polycaprolactone. The details of mixtures containing different amounts of QDs are listed in table **1**. Here the last column refers to the weight percentage of QDs defined with respect to the total weight including QDs, polymer and solvent. QDs (figure **2**(a)) were prepared by hot injection method, explained further in the Methods section. The particles were cleaned from excess ligands by mixing with acetone:methanol and followed by centrifugation. Figure **2**(b) presents the photograph of the solutions containing the QDs and polymer under UV light. Figure **2**(c) shows the QD loaded nanofiber mats after electrospinning on Al foils. Figure **2**(d) and **2**(e) show the high-angle annular dark field transmission electron microscopy image and scanning electron microscopy image of the QD loaded nanofiber respectively. The average diameter of the fibers is ~300 nm (see Supplementary data for the distribution of the diameter of the fibers).

(a) (b) (c)

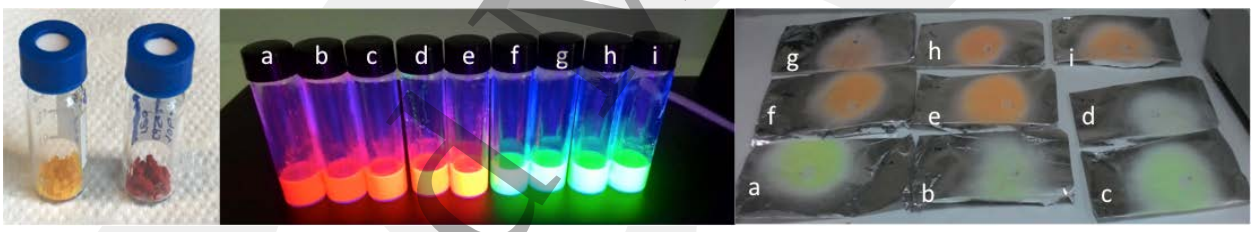

(d) (e)

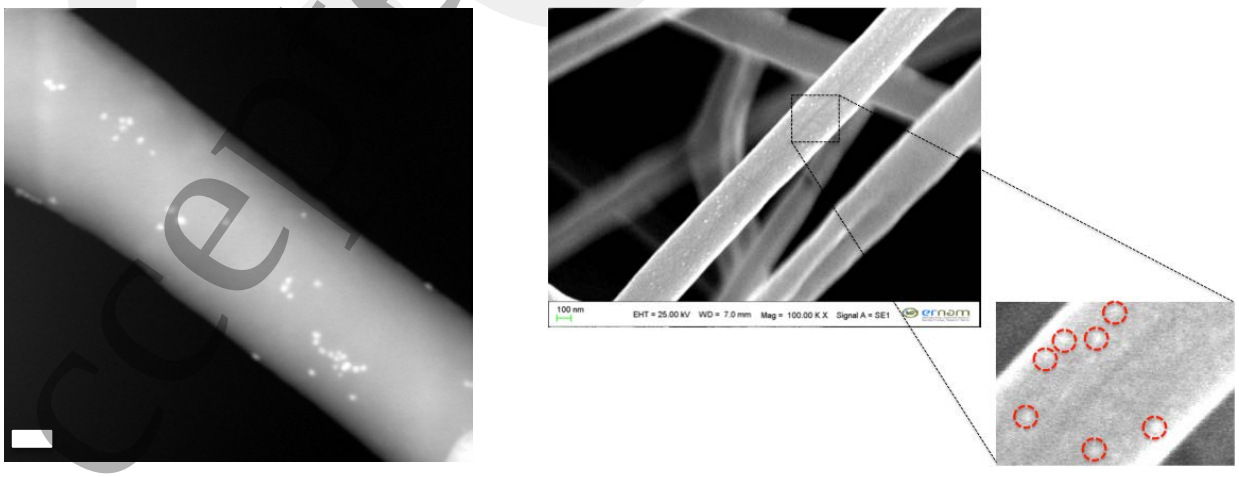

Figure 2. a) Dry powders of the green and red emitting QDs. (b) The photograph of the mixed QDs in solution (under UV exposure), (c) electrospun nanofiber mats loaded with QDs under day light (d) High-angle annular dark field transmission electron microscopy image of the QD loaded nanofiber (scale bar is 50 nm) (e) scanning electron microscopy image of the QD loaded nanofiber.

Table 1. The composition of QD embedded nanofibers

Label in Figure 3b	Sample content by weight QD_{Red}:QD_{Green}	Weight (mg) of red QD in 1.25 mL solvent	Weight (mg) of green QD in 1.25 mL solvent	Weight percentage of QD in the nanofiber
a	5:0	5	0	0.4
b	5:2.5	5	2.5	0.6
c	5:5	5	5.0	0.8
d	5:7.5	5	7.5	1.0
e	5:10	5	10	1.2
f	0:2.5	0	2.5	0.2
g	0:5	0	5	0.4
h	0:7.5	0	7.5	0.6
i	0:10	0	10	0.8

In order to observe the energy transfer among the colloidal nanocrystals in the nanofiber architecture we studied the time resolved photoluminescence spectroscopy of the QD loaded nanofibers. Figure **3**(a) and **3**(b) present the emission kinetics of the nanofibers loaded with varying ratios of the green and red emitting QDs and table **2** depicts the lifetime analysis of the nanofibers at a specific concentration ratio level (at the donor emission wavelength). The prepared nanofibers were characterized using time resolved photoluminescence measurement system, as a function of the ratio of the red and green QDs in the nanofiber. In the analysis of the fluorescence lifetime, the nanofiber mats were monitored at the donor emission wavelength in order to observe the effect of introducing the acceptor QDs in the medium. Starting with the red emitting QD loaded nanofibers, we introduced green emitting QDs in the proximity, and have observed the modification of the lifetime, due to the presence of the acceptor QD species. A multi exponential fitting is a commonly used fluorescence decay method to fit the fluorescence decay of quantum dots [24]. In the analysis, the lifetime decays were fit by using 3-exponentials (for donors) with the following relation:

$$I(t) = \sum_i^n A_i \exp(-t/\tau_i) \quad (2)$$

and

$$\tau_{amp} = \frac{A_1 \tau_1 + A_2 \tau_2 + A_3 \tau_3}{A_1 + A_2 + A_3} \quad (3)$$

where A_i is the amplitude of the lifetime decay corresponding to the individual τcomponent.

In our analysis, we used 0:2.5, 0:5, 0:7.5, and 0:10, (ratio of red to green QDs, will be denoted as "R:G" in the following text) sample as the control group of the study. Our results showed that by introducing donor QDs in the proximity of the acceptor QDs, the donor lifetime decays get faster. Namely, while the nanofiber containing only green QDs possesses amplitude-weighted lifetime of 9.30 ns, introducing the acceptor QDs in the medium with a concentration of "5:2.5", the lifetime value diminishes to 6.92 ns. This behavior is attributed to Förster type nonradiative energy transfer where the donor–green emitting QDs transfer their excitation energy in a nonradiative way to the acceptor-red emitting QDs in the nanofiber. In accordance, the FRET efficiency, ηhave been calculated using

$$\eta = 1 - \frac{\tau_{DA}}{\tau_D} \quad (2)$$

where, $\tau_{DA}$is the lifetime of the donor in the presence of the acceptor and $\tau_D$is the lifetime of the donor in the absence of the acceptor. Increasing the concentration of the donor QDs per acceptor QDs (red QD:green QD 5:5, 5:7.5, and 5:10), the average lifetime changed from 10.62ns to 7.02ns for 5:5, 10.70ns to 7.30ns for 5:7.5, from 12.46ns to 7.45ns for 5:10; which increased the FRET efficiency up to 40% in the case of concentrated donor-acceptor medium (see figure **3**(c)). It is worth noting here that as more and more donor QDs are introduced per fixed amount of

acceptor QDs, the lifetime values were shown to vary from 6.92ns (5:2.5) to 7.02ns for (5:5), to 7.30ns for (5:7.5) and to 7.45ns for (5:10). The decreasing trend in the donor lifetime quenching can be explained by the saturation of FRET efficiency with the introduction of more donors per acceptor species. The observed behavior presented in Fig. 3c, however is a combination of the homo-FRET among donor species and also FRET among donor-acceptor species, which takes into account the corresponding donor concentration as a control group. The control group decays of the donor emission as a function of the concentration are presented in figure **3**(b). The change in the lifetime decay is attributed to the homo-FRET, stemming from the energy transfer among the same type of the emitter.

(a) (b)

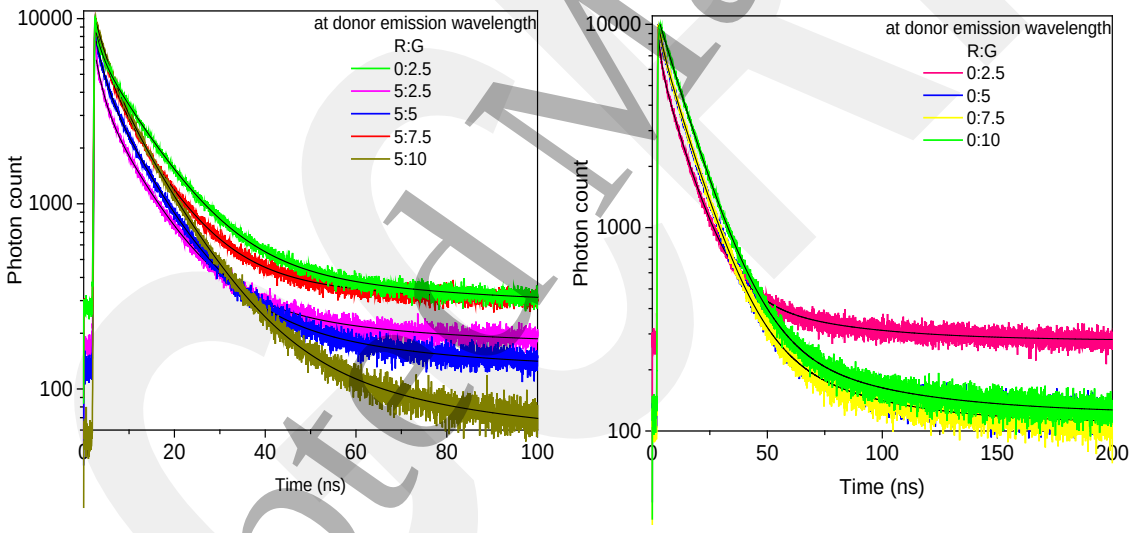

(c)

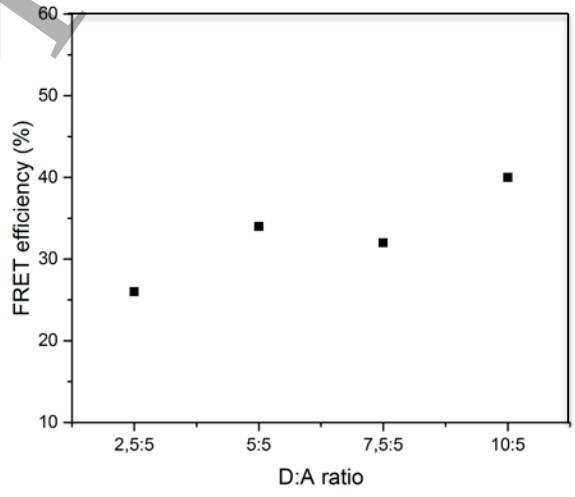

Figure 3. Time resolved photoluminescence decays of the nanofibers loaded with (a) red and green emitting QDs, by varying the red to green emitting QD ratio in the nanofiber (analysis at the donor emission wavelength) (b) green emitting QDs, corresponding to the same red to green emitting QD ratio in the nanofiber (analysis at the donor emission wavelength), (c) FRET efficiency calculated from donor lifetime quenching.

Table 2. Time resolved photoluminescence decay analysis (at the donor emission wavelength) of the nanofibers loaded with QDs

Red:Green ratio (Analysis @ 530 nm)	A_1	τ_1(ns)	A_2	τ_2 (ns)	A_3	τ_3 (ns)	$\tau_{average}$ (ns) (amplitude)
0:2.5	294.8 ±15.5	45.0 ±2.1	5914.2 ±63.7	10.0 ±0.1	1860 ±231	1.4±0.2	9.30
5:2.5	197.1 ±14	36.8 ±2.3	3298.7 ±53.7	8.8 ±0.1	2293 ±174	1.6±0.1	6.92
0:5	356.3 ±16.4	39.6 ±1.3	7759.7 ±66.5	10.9 ±0.1	1505 ±205	2.1±0.352	10.62
5:5	257.8 ±15.3	32.5 ±1.5	4366.4 ±58.6	8.8 ±0.1	2770 ±176	1.9±0.1	7.02
0:7.5	315.7 ±15.2	41.7 ±1.4	7923.3 ±66.3	11.1 ±0.8	1486 ±209	2.0±0.355	10.70
5:7.5	192.5 ±12.9	50.7 ±3.1	5141.9 ±64.7	9.1 ±0.1	3400 ±183	2.1±0.1	7.30
0:10	229.4 ±12.1	53.9 ±2.1	3122.1 ±56.3	14.1 ±0.2	6486.1 ±75	10.2±0.104	12.46
5:10	235.6 ±13.6	34.3 ±1.3	5441.4 ±61.9	9.5 ±0.1	3713 ±164	2.7±0.1	7.45

Figure **4** shows the emission kinetics of the acceptor QDs when loaded with donor QDs in close proximity. In the acceptor lifetime analysis, we have used a double exponential fitting of the lifetime, given as

$$\tau_{amp} = \frac{A_1 \tau_1 + A_2 \tau_2}{A_1 + A_2} \quad (4)$$

As compared with the lifetime of the bare acceptor QDs, as more and more donors are introduced to the medium, the lifetime values have been shown to be prolonged from 9.74 ns to 10.24 for 5:2.5, to 11.46 for 5:5, to 12.80 for 5:7.5 and to 13.54 ns for 5:10 (See table **3**). The energy feeding to the acceptor QDs as a result of FRET can be viewed by focusing to the first few tens of nanoseconds of the decay in the acceptor photoluminescence decay curves. The observed trend is in agreement with the FRET based light harvesting system in a sense that from the acceptor point of view, more donors in the medium would increase the energy feeding per acceptor species.

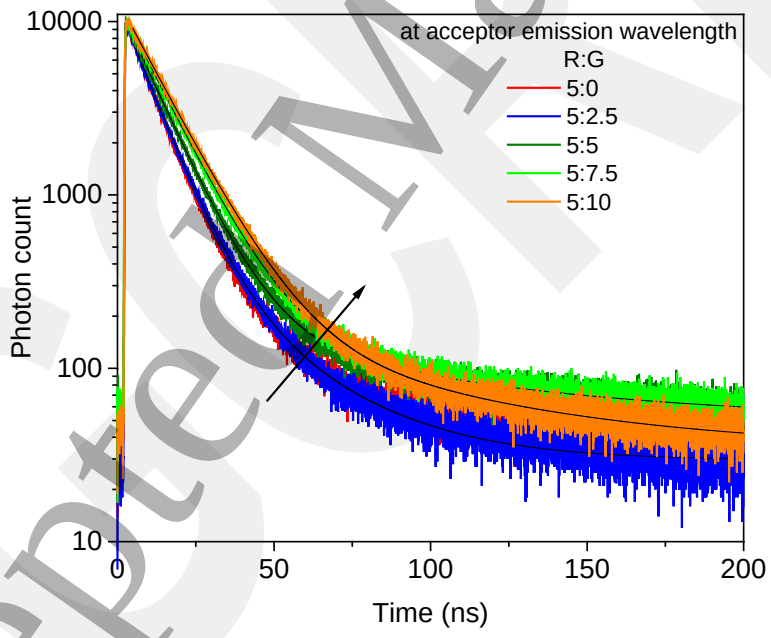

Figure 4. Time resolved photoluminescence decays of the nanofibers loaded with red and green emitting QDs, by varying the red to green emitting QD ratio in the nanofiber (analysis at the acceptor emission wavelength).

Table 3. Time resolved photoluminescence decay analysis (at the acceptor emission wavelength) of the nanofibers loaded with QDs

Red:Green ratio (Analysis@630 nm)	A_1	τ_1(ns)	A_2	τ_2 (ns)	$\tau_{average}$ (amplitude) (ns)
5:0	409.1±17.8	29.3±0.8	8139.9±74.8	8.8±0.1	9.74
5:2.5	499.4±19	28.3±0.7	7678.4±72.9	9.1±0.1	10.24
5:5	223.7±11.3	45.6±1.7	7777.4±64.3	10.5±0.1	11.46
5:7.5	150.2±7.6	70.7±2.8	9026.9±66.9	11.8±0.1	12.80
5:10	200.1±8.9	60.3±1.9	8898.7±63.9	12.5±0.1	13.54

We further studied the steady state emission kinetics of the nanofibers loaded with QDs. In that regards, figure **5** shows the change in the steady state emission of the green only, red only and mixed (red to green ratio of 5:5) QD nanofiber samples. The intensity of the green emitting nanofiber has decreased to 71% of its initial intensity (integrated area under the curve), which leads to 52% enhancement of the emission of the red emitting QDs in nanofiber.

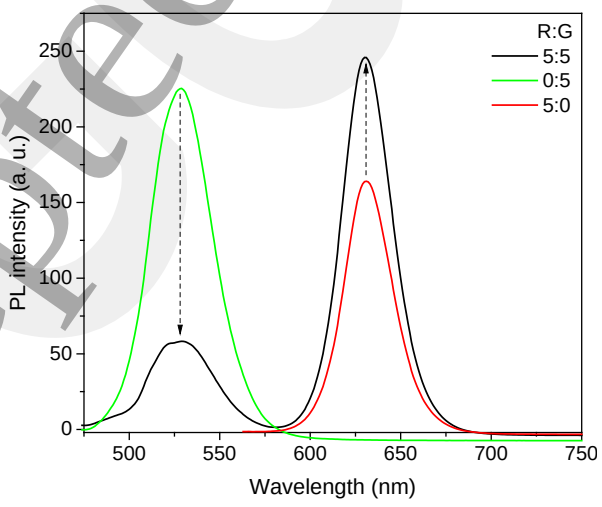

Figure 5. Steady state photoluminescence spectra of the donor only (R:G: 0:5), acceptor only (R:G: 5:0) and mixed film (R:G:5:5)

The enhancement of the acceptor emission due to FRET is lower as compared with the observed decrease in the donor emission. This is attributed to quantum efficiency of the acceptor in the nanofiver as well as the phononic vibrations as a potential loss mechanism in the nonradiative energy transfer channel.

The loading of the QDs in the nanofiber architecture allows for hybridization of the nanofibers with the blue LED, allowing for the achievement of the white light. It is known that, in the 3 color (blue, green, red) approach, the narrow emitters cannot possess very high performance of the color rendering index (CRI) since the spectrum cannot span the entire spectrum in 3 color mixing approach. We have simulated the potential performance of the white light-emitting platform using green emitting nanofiber with 538.5 nm emission peak and 38nm FWHM and red emitting nanofiber with 632.5 nm along with 35 nm FWHM. Our results show that theoretically the maximum achievable color rendering index (CRI) is 62 for a correlated color temperature (CCT) value <4000K, using the intensity levels of 4% blue, 45% green and 51% red emission (Figure **6**(a)). In this analysis we have varied the intensity values of the 3 primaries using their experimental peak emission position and full width half maximum values. Therefore, in that aspect we have simulated the intensities and then use that information to experimentally mimic the optimal white light. In this context, we have integrated green emitting nanofiber (R:G:0:5) and (R:G:5:2.5) nanofibers on commercially available blue LED and achieved CRI value of 60, correlated color temperature (CCT) of 3632.5K and luminous efficacy of optical radiation (LER) value of 307.7 lm/W_{opt} (Figure **6**(b)), corresponding to CIE coordinates of (x,y)=(0.4186, 0.4462). The photograph of the prepared QD loaded nanofibers are given in Figure **6**(c), the actual hybridized platform of nanofibers under daylight is given in Figure **6**(d) and the operational white light-emitting device under dark is given in Figure **6**(e), respectively.

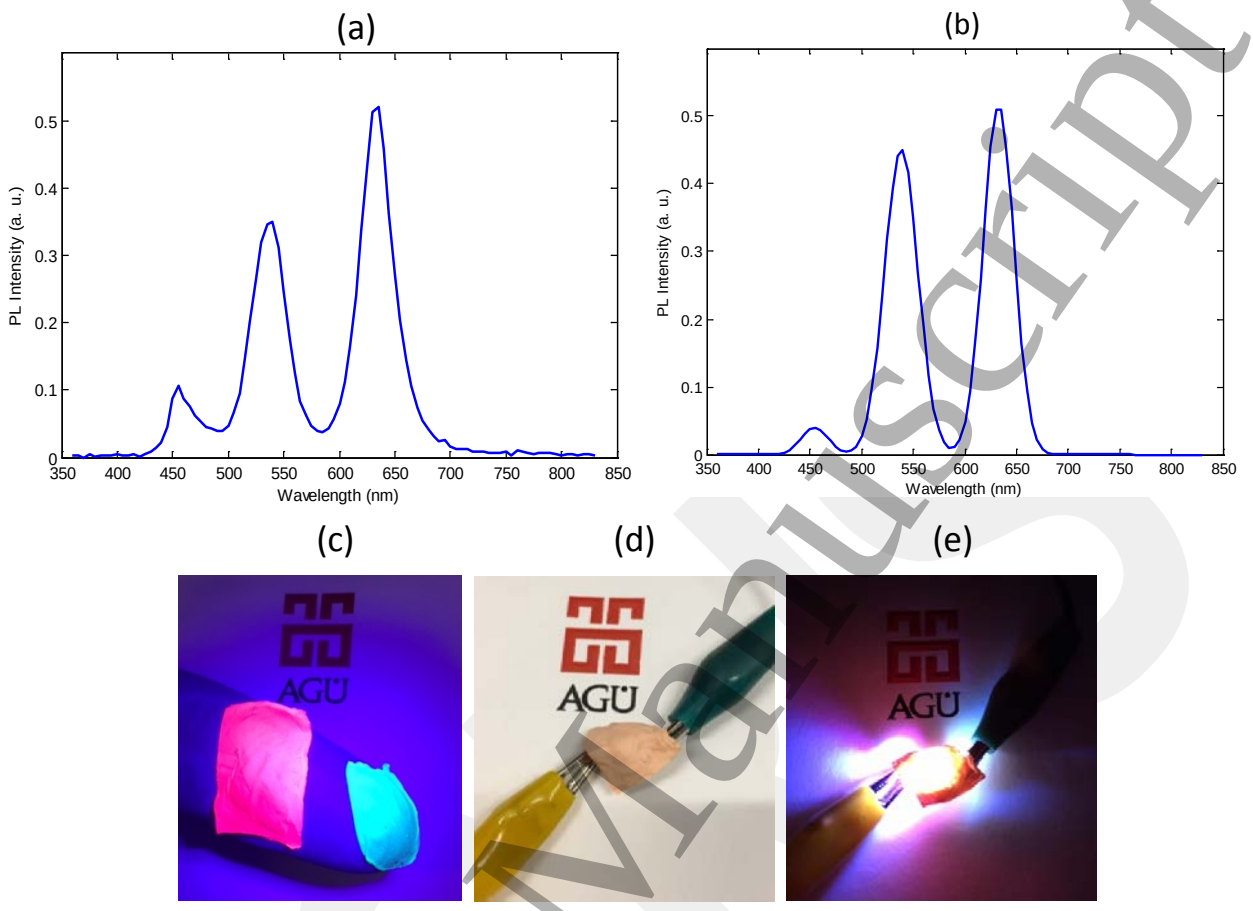

Figure 6. (a) Experimental spectrum of the blue LED integrated QD loaded nanofibers (b) Theoretical simulation of the amplitudes of the blue LED and QD loaded nanofibers (c) the photograph of the QD loaded nanofibers under UV exposure, (d) the photograph of the QD loaded nanofibers hybridized with blue LED, (e) the photograph of the white light emitting device under operation.

4. Conclusions

In conclusion, this work demonstrated the fabrication of electrospun 1D nanostructures loaded with green and red emitting CdSe/ZnS QDs. We have extensively studied the energy transfer among the particles that are spatially confined in nanofiber architecture and present the modification of the lifetime of the donor acceptor pairs upon the resonance energy transfer. Furthermore, we have demonstrated the first QD-nanofiber blends for surface integrated blue

LED application to generate energy transfer assisted white light. Our results provide in depth understanding of the light harvesting of the colloidal 0D particles that are spatially confined in a quasi 1D platform, which would potentially open up new pathways towards surface emitting platforms with high surface to volume ratio.

Supplementary Data: Details of experiments which are carried out to obtain highly efficient colloidal red and green QD, TEM analysis, XRD and XPS measurements of synthesized QDs, detailed and the distribution of the diameters for fibers electrospun from solutions are available in the online version of this article.

Acknowledgements

EM acknowledges financial support from TUBITAK project no's 114E107 and MSO acknowledges financial support from TUBITAK project no 115M517.

References

[1] Anikeeva P O, Halpert J E, Bawendi M G and Bulović V 2009 Quantum Dot light-emitting devices with electroluminescence tunable over the entire visible spectrum. *Nano Lett*. **9** 2532–6.

[2] Demir H V, Nizamoglu S, Erdem T, Mutlugun E, Gaponik N, Eychmüller A 2011 Quantum dot integrated LEDs using photonic and excitonic color conversion *Nano Today* **6** 632-47.

[3] Luo Z, Xu D, Wu S-T 2014 Emerging Quantum Dots Enhanced LCDs *J. of Display Tech*. **10** 526 – 39.

[4] Sohn I S, Unithrattil S, Im W B 2014 Stacked Quantum Dot Embedded Silica Film on a Phosphor Plate for Superior Performance of White Light-Emitting Diodes *ACS Appl. Mater. Interfaces* **6**, 5744–8.

[5] Jang E, Jun S, Jang H, Lim J, Kim B, Kim Y 2010 White-Light- Emitting Diodes with Quantum Dot Color Converters for Display Backlights *Adv. Mater.* **22** 3076–80.

[6] Kim B H *et al* 2015 High-resolution patterns of quantum dots formed by electrohydrodynamic jet printing for light-emitting diodes *Nano Lett.* **15** 969-73.

[7] Kagan C R, Lifshitz E, Sargent E H, Talapin D V 2016 Building devices from colloidal quantum dots *Science* **353** 6302.

[8] Klar B T A, Franzl T, Rogach A. L and Feldmann J 2005 Super-efficient exciton funneling in layer *Adv. Mater.* **17** 769- conductor nanocrys
73.

[9] Yang H Y, Fu Y, Jang M S, Li Y, Lee J H, Chae H and Lee D S 2016 Multifunctional Polymer ligand Interface CdZnSeS/ZnS Quantum Dot/Cy3-labeled Protein pairs as sensitive FRET sensors *ACS Appl. Mater. Interfaces.* **8** 35021–32.

[10] Clapp A R *et al* 2007 Two-Photon Excitation of Quantum-Dot-Based Fluorescence Resonance Energy Transfer and Its Applications *Adv. Mater.* **19** 1921-6.

[11] Meng C, Xiao Y, Wang P, Zhang L, Liu Y, Tong L 2011 Quantum-Dot-Doped Polymer Nanofibers for Optical Sensing *Adv. Mater.* **23** 3770–4.

[12] Yang X, Xu R, Bao D, Li B 2014 Gold Nanorod-Enhanced Light Emission in Quantum-Dot-Doped Polymer Nanofibers *ACS Appl. Mater. Interfaces* **6** 11846−50.

[13] Aykut Y, Saquing C D, Pourdeyhimi B, Parsons G N, Khan S A 2012 Templating Quantum Dot to Phase-Transformed Electrospun TiO2 Nanofibers for Enhanced Photo-Excited Electron Injection *ACS Appl. Mater. Interfaces* **4** 3837−45.

[14] Zhang R, Yu H, Li B 2012 Active Nano waveguides in Polymer Doped with CdSe-ZnS Core-Shell Quantum Dots *Nanoscale* **4** 5856−9.

[15] Liu H, Edel J B, Bellan L M, Craighead H 2006 Electrospun Polymer Nanofibers as Subwavelength Optical Waveguides Incorporating Quantum Dots *Small* **2** 495−9.

[16] Yu H, Zhang R, Li B 2011 Optical Properties of Quantum-Dot Decorated Polymer Nanofibers *Nanotechnology* **22** 335202.

[17] Kim N, Na W, Yin W, Jin H, Ahn T K, Cho S M and Chae H 2016 CuInS2/ZnS quantum dot-embedded polymer nanofibers for color conversion films *J. Mater. Chem. C*. **4** 2457.

[18] Tetsuka H, Nagoya A and Asahi R 2015 Highly luminescent flexible amino-functionalized graphene quantum dots@cellulose nanofiber–clay hybrids for white-light emitting diodes *J. Mater. Chem. C* **3** 3536.

[19] Choi Y J, Hwang D, Chung H, Kim D Y, Kim D 2015 Controlling the spatial distribution of quantum dots in nanofiber for light-harvesting devices *NPG Asia Materials* **7** 1-7.

[20] Altintas Y, Genc S, Talpur M Y, Mutlugun E 2016 CdSe/ZnS quantum dot films for high performance flexible lighting and display applications *Nanotechnology* **27** 295604.

[21] Bae W K, Char K, Hur H, Lee S 2008 Single-step synthesis of quantum dots with chemical composition gradients *Chem. Mater.* **20** 531-9.

[22] Bae W K, Kwak J, Lim J, Lee D, Nam M K, Char K, Lee C, Lee S 2010 Multicolored Light-Emitting Diodes Based on All- Quantum-Dot Multilayer Films Using Layer-by-Layer Assembly Method *Nano Lett.* **10** 2368−73.

[23] Lim J, Jun S, Jang E, Baik H, Kim H, Cho J 2007 Preparation of highly luminescent nanocrystals and their application to light-emitting diodes *Adv. Mater.* **19**, 1927-32.

[24] Xu H, Chmyrov V, Widengren J, Brismar H, Fu Y 2015 Mechanisms of fluorescence decays of colloidal CdSe–CdS/ZnS quantum dots unraveled by time-resolved fluorescence measurement Phys. Chem. Chem. Phys. **17** 27588-27595.